16th World Conference on Earthquake Engineering, 16WCEE 2017
Santiago Chile, January 9th to 13th 2017
Paper N° 4948
Registration Code: S-A1463505141

Spectral-Analysis-of-Surface-Waves (SASW) Testing to Evaluate V_S Profiles at Geotechnical and Geological Sites

K.H. Stokoe, II(1), S. Hwang(2), and S.-H. Joh(3)

(1) *Professor; Jennie C. and Milton T. Graves Chair in Engineering, Department of Civil, Architectural and Environmental Engineering, University of Texas at Austin, U.S.A., k.stokoe@mail.utexas.edu*
(2) *Graduate Research Assistant, Civil, Architectural, and Environmental Engineering Department, University of Texas at Austin, U.S.A., syongmoon@utexas.edu*
(2) *Professor; Civil, and Environmental Engineering Department, Chung-Ang University, Republic of Korea., shjoh@cau.ac.kr*

Abstract

The Spectral-Analysis-of-Surface-Waves (SASW) testing method is a nondestructive and nonintrusive seismic method. The method utilizes the dispersive nature of Rayleigh-type surface waves propagating through a layered material to evaluate the shear wave velocity profile. Dispersion in surface wave velocity arises from changing stiffness properties with depth. SASW field testing involves generating surface waves at one location on the exposed material surface and simultaneously measuring the motions perpendicular to the surface created by the passage of surface waves between multiple pairs of surface receivers. All measurement points are arranged along a radial path from the source. Successively larger spacings between receiver pairs and between the source and first receiver are used to measure progressively longer wavelengths. The profiling depth generally equals about one-half of the longest wavelength which also corresponds to the largest spacing between receiver pairs. Spectral analysis is used to separate the waves by frequency or wavelength to determine the experimental ("field") dispersion curve of the site. A forward modeling or inversion procedure is then used to approximate the field dispersion curve with a one-dimensional system of horizontal layers with varying stiffnesses and thicknesses. The dynamic stiffness matrix method is the modeling algorithm used in the matching or inversion process. SASW measurements are illustrated using four example projects with V_S profiles ranging in depths from 5 to 450 m. For the deeper profiling, a large hydraulically-operated mobile shaker, called Liquidator, was used.

Keywords: SASW seismic testing, surface wave dispersion, example site investigations, deep V_S profiling, mobile shaker

1. Introduction

The Spectral-Analysis-of-Surface-Waves (SASW) method was introduced in the 1980's by researchers at the University of Texas in Austin (Nazarian and Stokoe 1984 [1] and Stokoe and Nazarian 1985 [2]). The SASW method is a nondestructive and nonintrusive seismic method that evolved from the steady-state Rayleigh-wave method discussed in Richart et al. 1970 [3]. The method involves using active surface sources to generate Rayleigh-type surface waves and surface receivers to monitor the passage of these waves along a linear array. The objective of the field measurements is to determine phase velocities of Rayleigh waves over a wide range in frequencies or wavelengths (typically more than two orders of magnitude). The SASW method was developed to perform faster, more efficient and more accurate measurements than any previous surface-wave method at that time (early 1980s). The field testing incorporated new, portable, digital equipment for recording and performing real-time frequency analysis and phase measurements between pairs of surface receivers as well as real-time viewing of the phase for quality control. In addition, the dynamic stiffness matrix method developed by Kausel and Roesset 1981[4] became the theoretical basis for modeling the field dispersion curve of phase velocity versus wavelength from which the shear wave velocity (V_S) profile of the site is determined. An overview of the SASW method is initially presented using one example project. Three additional examples are then presented to illustrate the field measurements, modeling field dispersion curves and resulting V_S profiles. These examples are also presented to show a wide range of applications.

2. Overview of SASW Test Method

The SASW method utilizes the dispersive nature of Rayleigh-type surface waves propagating through a layered material to evaluate the shear wave velocity profile of the material (Stokoe et al 1994 [5]). In this context, dispersion arises when surface wave velocity varies with wavelength or frequency. Dispersion in surface wave velocity arises from changing stiffness properties of the soil and rock layers with depth. This phenomenon is illustrated in Fig.1 for a multi-layered solid. A high-frequency surface wave, which propagates with a short wavelength, only stresses material near the exposed surface and thus only samples the properties of the shallow, near-surface material (Fig.1b). A lower-frequency surface wave, which has a longer wavelength, stresses material to a greater depth and thus samples the properties of the shallower and deeper materials (Fig.1c). Spectral analysis is used to separate the waves by frequency or wavelength to determine the experimental ("field") dispersion curve for the site as illustrated in Fig.1d. A forward modeling procedure is then generally used to calculate theoretical dispersion curve that fits the field dispersion curve with a one-dimensional layered system of varying layer stiffnesses and thicknesses (Joh 1996 [6]). The one-dimensional shear wave velocity profile that generates a dispersion curve which most closely fits the field dispersion curve is often presented as the shear wave velocity profile. However, due to the non-uniqueness of the surface wave inverse or forward-modeling problem, a family of V_S profiles which fit within the uncertainty bounds of the field dispersion data should be considered in future studies as discussed by DiGiulio et al 2012 [7] and Cox and Teague 2016 [8].

The SASW testing process involves using active sources to generate surface waves at one location on the exposed material surface while simultaneously measuring vertical motions on the surface created by the passage of surface waves between pairs of receivers. The normal testing configuration consists of a source and two receiver pairs oriented in a linear array as illustrated in Fig.2. In this configuration, called the common-middle-receiver geometry, the middle receiver (R2) is located at the centerline of the test array and is not moved during testing, assuming no space constraints. The distance (x) between the source and receiver R1 is kept equal to the distance (x) between receivers R1 and R2 in the first pair as shown in Fig.2. At the same time, the middle receiver (R2) is used as the first receiver in the second receiver pair (receivers R2 and R3). In this case, the distance (2x) between the source and first receiver in the second pair equals the distance (2x) between the two receivers in the second receiver pair. Using this source-receiver configuration, successively longer spacings between receiver pairs and between the source and first receiver in each pair are used to measure progressively longer wavelengths. Testing is performed with multiple (typically 8 or more) sets of source-receiver spacings (x, 2x, 4x, 8x, etc.), depending on the profiling depth and lateral variability inferred by viewing the dispersion data during field measurements. The totality of all sets of source-receiver spacings is called an SASW array.

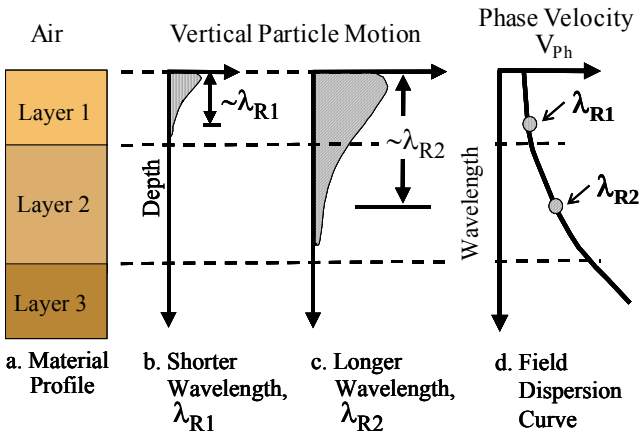

Fig.1 – Illustration of surface waves with different wavelengths sampling different materials in a layered system that results in dispersion in phase velocity, V_{Ph}. [9]

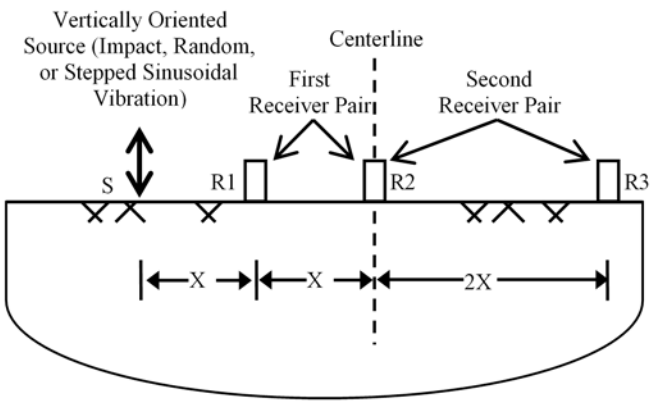

Fig.2 – Common-Middle-Receiver geometry generally used in SASW testing (Note: Location of receiver (R2) remains fixed)

The variation in phase shift with frequency is recorded for surface waves propagating between each receiver pair. The phase velocity is calculated at each frequency using the relationship $V_{Ph} = (f\,(360/\phi)\times d)$ in which V_{Ph} is the phase velocity in m/s, f is the frequency in Hertz (cycles per sec), ϕ is the phase angle in degrees (at frequency f), and d is the distance between the receivers in the pair in meters. From this calculation, a plot of phase velocity versus frequency, called an individual dispersion curve, is generated for each receiver pair. This procedure is repeated for all source-receiver spacings used at the site and involves significant overlapping in the dispersion data between adjacent receiver pairs. The individual dispersion curves from all receiver pairs are combined into a single composite dispersion curve called the "field", "global", or "experimental" dispersion curve. The field dispersion is also considered the "signature of the site" which represents the global nature of these measurements at most geological sites compared with the localized nature of seismic measurements using boreholes. This process is illustrated in Section 3.3.

Once the composite field dispersion curve is generated, an iterative forward modeling procedure or an inversion procedure is used to create a theoretical dispersion curve that matches the experimental dispersion curve. The software program named, WinSASW [6], or an equivalent software is used for this purpose. WinSASW uses an algorithm that is based on the stiffness-matrix approach [4] to generate a theoretical dispersion curve for a given shear wave velocity profile. The theoretical dispersion curve is generated using a complete solution that includes all modes and both surface and body waves (termed the 3D approach) (Foinquinos 1991 [10], Roesset et al 1991 [11] and Lin et al 2014 [12]). With the iterative procedure, an initial shear wave velocity profile is first assumed based on the characteristics of the measured experimental dispersion curve. A theoretical dispersion curve is generated and compared with the experimental curve. The features of the shear wave velocity profile (wave velocities and layer thicknesses) are iteratively changed until an acceptable fit between the theoretical and experimental curve is achieved. The "goodness of fit" is generally based on visually determining a best fit based on the combined judgements and experiences of the experts performing the tests. This process is illustrated in Section 3.4. Sometimes, the inversion process in WinSASW is used to confirm and/or refine the V_S profile determined by forward modeling.

3. Example Field Testing and Analysis Procedures

3.1 Field Equipment and Testing Procedures

The active-source SASW testing that was performed in the examples presented in this paper involved three different types of sources and two different types of receivers. In terms of active sources, the simplest and least energetic source is some type of hand-held hammer such as the sledge hammer shown in Fig.3a. The sledge hammer is used to apply transient, vertical impacts to the exposed surface. Hammer sources are mainly used at short spacings, generally less than 5 m at soil sites and less than 10 m at rock sites. The second type of source is a random noise generator such as the bulldozer shown in Fig.3b. The bulldozer is used to move continuously back and forth over distances of 3 to 5 m at one end of the array as illustrated in Fig.3c. Quick stops and starts are important in generating lower frequencies, say 2 to 5 Hz. Also, in the writers' experience, steel-tracked bulldozers are better generators of lower frequencies than large drop weights. The third type of source is a large vibroseis. The one-of-kind, low-frequency vibroseis named Liquidator that is operated by the University of Texas is shown in Figure.3d. Liquidator is operated in a downward, stepped-sine sweeping mode as illustrated in Fig.3e.

The two types of receivers are accelerometers and vertical velocity transducers (commonly called vertical geophones). Accelerometers are used on high-stiffness materials such as rock, concrete or pavements as discussed subsequently in the second example. At soil sites or sites with soil over rock, vertical velocity transducers are used. In this case, 4.5-Hz or 1-Hz geophones are used, depending on the frequency content of the signal. Generally, 4.5-Hz geophones have a usable frequencies range from about 1 Hz to above 1000 Hz. On the other hand, 1-Hz geophones have an operating range from 0.3 to 500 Hz and a calibration factor (output) about ten times a 4.5-Hz geophone. In the testing shown in Fig.3a, 1-Hz geophones are being used.

3.2 Spectral Calculations

A dynamic signal analyzer is used in the field to measure time-domain records (x(t) and y(t)) from the two receivers

(a) Sledge hammer often used at short (< 5 m) receiver spacings

(b) Bulldozer used as a high-energy source for moderate (< 75 m) profiling

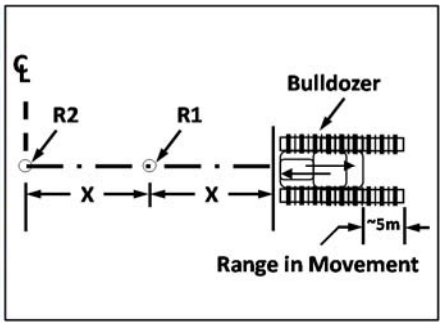

(c) Typical back-and-forth movement of bulldozer

(d) Liquidator used as a low-frequency source for deep profiling (depths > 300 m)

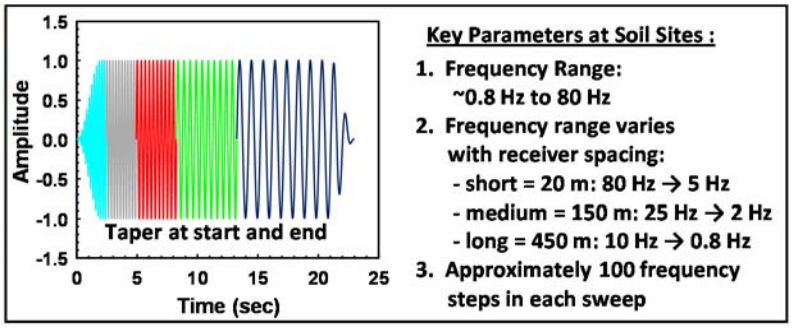

(e) Illustration of stepped-sine sweep with Liquidator which can last for less than 1 minute to more than 30 minutes

Fig. 3 – Active sources used in performing SASW field testing

in each receiver pair. These time records are then transformed into the frequency domain (X (f) and Y (f)) and used to calculate the power spectra (G_{XX} and G_{YY}) and the cross power spectrum (G_{XY}) as follows:

$$G_{XX} = X^*(f) \bullet X(f) \quad (1)$$

$$G_{YY} = Y^*(f) \bullet Y(f) \quad (2)$$

$$G_{XY} = X^*(f) \bullet Y(f) \quad (3)$$

$$\phi(f) = \arctan \bullet \frac{\mathrm{Im}(G_{XY})}{\mathrm{Re}(G_{XY})} \quad (4)$$

where $G_{XY}(f) = \frac{1}{N}\sum_{i=1}^{N} X^*(f) \bullet Y_1(f)$ is the cross power spectrum from coherent signal averaging, (*) represents the complex conjugate of the quantity, Im signifies the imaginary part of the expression, Re signifies the real part of the expression, and $\phi(f)$ is the relative phase of the cross power spectrum between the pair of receivers.

The relative phase from the cross power spectrum $\phi(f)$ is the key spectral quantity in SASW testing. The spectral functions are determined using signal averaging. The number of averages varies with source type and averaging is concluded once a stable average is reached as determine by viewing the record in real time. Five averages are often used when the sledge hammer is employed. When Liquidator is used, a stepped sinusoidal loading is used (Fig.3d) with three averages at shorter spacings and more averages (5 or more) at longer spacings. The relative phase of the cross spectrum, simply called the phase hereafter, represents the phase difference between the motions measured by the receiver pair. An example of the wrapped phase spectrum from one receiver pair is shown in Fig.4a. These data were collected using Liquidator as the source and 366-m spacings between source and R1 and between the receiver pair. These data were collected at a site in West Texas where seismic response analyses were required in a site application. This site is referred to as Example #1 hereafter.

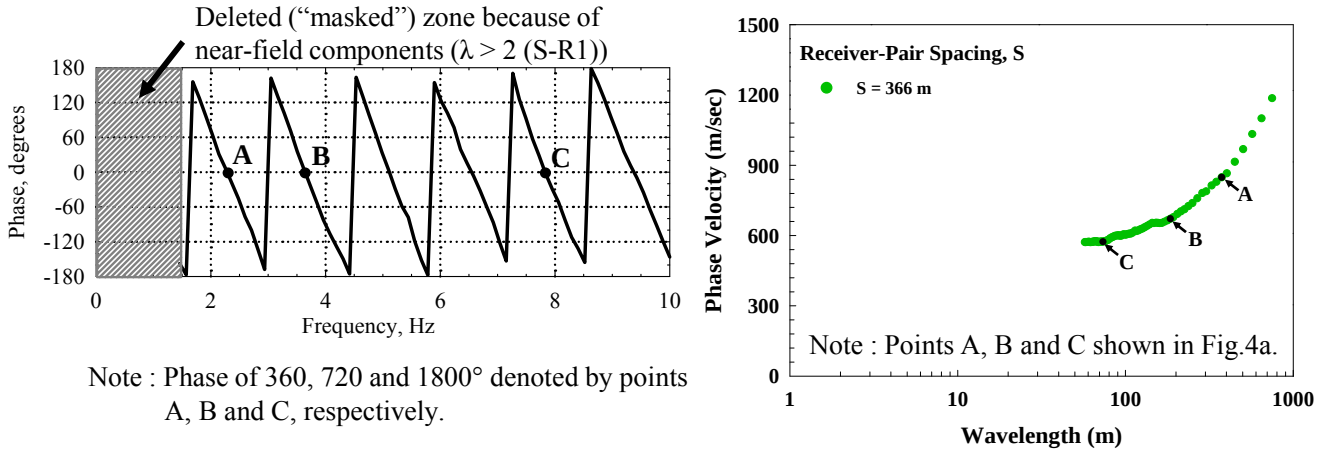

(a) Wrapped phase calculated from the cross-power spectrum

(b) Individual experimental dispersion curve created from Fig.4a

Fig. 4 – Phase of the cross power spectrum and resulting individual dispersion curve: Liquidator as the seismic source and receiver pair with a spacing of 366 m at the West Texas Example #1 site

3.3 Construction of Individual and Composite Field Dispersion Curves

Construction of an individual dispersion curve from each receiver pair involves loading the wrapped phase plots into the program WinSASW [6]. A masking procedure is then performed to manually eliminate portions of the data with poor signal quality and/or portions of the data with near-field waveform components. In Fig.4a, the masking applied to the phase plot is shown. In this example, the only portion of the record assumed to be potentially distorted is that portion consider to include near-field data which is marked by the darkened zone from 0 to 1.46 Hz. The near-field data are assumed to be composed of wavelengths longer than twice the spacing of the receiver pair, hence, $\lambda > 732$ m. (This criterion can also be expressed as wavelengths greater than twice the S-R1 distance.) The masking information is used in the WinSASW program to unwrap the phase plot, and then calculate the individual dispersion curve.

As an example of the process followed in constructing an individual dispersion curve, consider Points A, B and C in Fig.4a. Points A, B and C represent seismic waves with one, two and five wavelengths between the receivers, respectively. The unwrapped phase angles are 360° (one wavelength), 720° (two wavelengths) and 1800° (five wavelengths). The frequencies associated with Points A, B and C are 2.3, 3.6 and 7.8 Hz, respectively, which results in phase velocities of 842, 659 and 571 m/s, respectively. The complete individual dispersion curve calculated from the unmasked portion of the wrapped phase record in Fig.4a is shown in Fig.4b. This process is repeated for all receiver spacings which results in a composite experimental (field) dispersion curve that covers a wide range of wavelengths. The composite experimental dispersion curve for the West Texas site using a sledge hammer and Liquidator as the seismic sources is shown in Fig.5a. The maximum wavelength, λ_{max}, measured at the site was 730 m. This wavelength was measured with S-R1 = 183 m and R2 - R3 = 366 m. In this case, the wrapped- phase record was well conditioned and phase data were used beginning at a wrapped phase of 160˚. (As noted above, unwrapping of phase records generally begins at 180˚.) The maximum depth to which the V_S profile was determined at this site with Liquidator is $\lambda_{max}/2$ or 365 m as discussed below.

3.4 – Forward Modeling and Resulting V_S Profile

With the composite field dispersion curve shown in (Fig.5a), an iterative forward modeling procedure is used to determine a V_S profile by matching the field dispersion curve with a theoretically-determined dispersion curve. Apparent phase velocities are measured in SASW field testing. These velocities correspond to the superposed modes of fundamental and higher-mode surface waves and body waves. The forward modeling algorithm normally used in the SASW analysis is the 3-D global model in WinSASW ([6], [11] and [12]). In this model, the first and second receivers in the receiver pair are assumed to be located at 2 λ and 4 λ from the source, respectively; hence, far-field measurements. The theoretical dispersion curve using the 3-D global model was fit to the West Texas

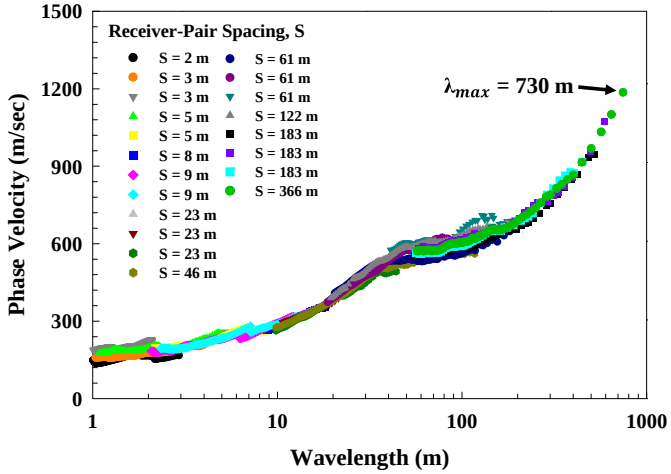

(a) Composite experimental (Field) dispersion curve evaluated from 20 receiver pairs

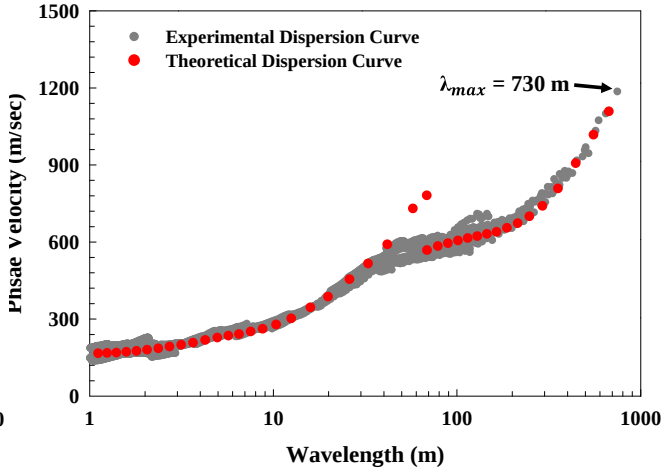

(b) Forward modeling fit shown in terms of a V_{Ph} – log λ plot

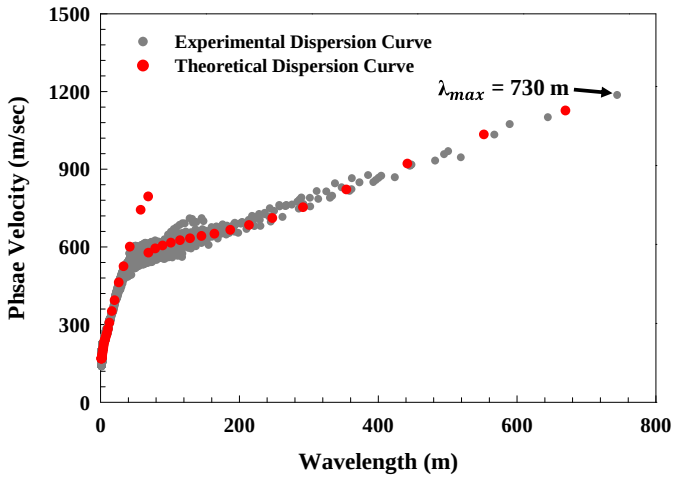

(c) Forward modeling fit shown in terms of a V_{Ph} – λ plot

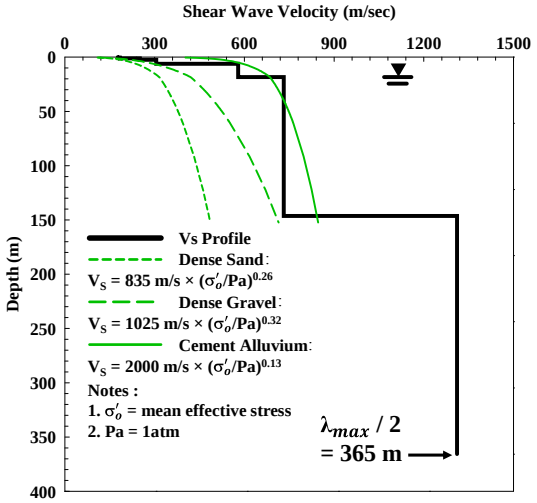

(d) V_S Profile evaluated to 365m with 3 reference profiles for comparison

Fig. 5 –Composite experimental dispersion curve, forward-modeling fit of the theoretical dispersion curve based on 3-D global modeling and resulting V_S profile for the West Texas Example #1 site

field dispersion curve and the results are shown in Figs.5b and 5c. In Fig.5b, the V_{Ph} – log λ plot permits the dispersion data with short-to-moderate wavelengths to be easily examined. In Fig.5c, the V_{Ph} – λ plot permits the dispersion data with moderate-to-long wavelengths to be easily examined. This combination of two plots allows one to judge more easily the data quality and the completeness of the fit. Clearly, the fit is robust and there is at least one shift between modes in the wavelength range of about 40 to 70 m. The resulting V_S profile is presented in Fig.5d and is tabulated in Table 1.

The resulting V_S profile in Fig.5d for the West Texas site was quite straightforward to evaluate even though there was a shift between modes as noted above. The site is normally dispersive, and reasonably laterally uniform as shown by little variability around a robust trend in the field dispersion data. The generalized geological model of stiff (possibly cemented) soil over moderately stiff rock is supported by comparison with the reference V_S profiles of dense sand, dense gravel and cemented alluvium that are plotted to a depth of 150 m in Fig.5d. The moderately stiff rock (V_S~1300 m/s) occurs at a depth of about 150 m. The V_S profile is presented to a depth of 365 m which equals λ_{max} / 2 and also equals the maximum R2-R3 spacing.

Table 1 – Profile parameters used to develop theoretical dispersion curve shown in Figs.5b and 5c

Layer No.	Layer Thickness, m	Depth to Top of Layer, m	S-Wave Velocity, m/s	Assumed Poisson's Ratio	P-Wave Velocity, m/s	Assumed Total Unit Weight, t/m^3
1	0.40	0.00	177	0.33 $^{\nabla}$	351	1.9
2	0.67	0.40	183	0.33 $^{\nabla}$	363	1.9
3	1.37	1.07	250	0.33 $^{\nabla}$	496	1.9
4	3.66	2.44	305	0.33 $^{\nabla}$	605	1.9
5	12.19	6.10	579	0.33 $^{\nabla}$	1150	2.0
6	128.02	18.29	732	0.35	1524 ^{X}	2.1
7	213.70	146.30	1311	0.33	2602 $^{\Delta}$	2.1
8*	Half Space	360	1311	0.33	2602 $^{\Delta}$	2.1

$^{\nabla}$ Assumed Poisson's ratio for stiff soil above water table.
^{X} Assumed P-wave velocity for stiff soil below the water table.
$^{\Delta}$ Assumed Poisson's ratio for rock; * Layer extends below maximum depth (λ_{max} / 2) of the V_S profile.

4. Example #2 – Evaluation of a Concrete-Lined Tunnel and Surrounding Host Rock

Many uses of V_S profiles evaluated with the SASW method have involved profiling constructed systems and their geotechnical foundation materials to assist in engineering analyses and forensic studies as well as seismic site response studies. A forensic study of a concrete-lined tunnel in rock is discussed in this example. A generalized cross section of the tunnel is shown in Fig.6a. The tunnel has an inside diameter of about 3.5 m, with a concrete liner that was designed to have a nominal thickness of 30 cm. An extensive investigation was conducted in which SASW testing was performed at more than 100 locations along the longitudinal axis of the tunnel. SASW testing was performed with hand-held hammers as sources and accelerometers as receivers. The accelerometers were held magnetically to metal disks that were glued to the concrete liner before testing in a pre-selected array configuration. This general configuration is illustrated in Fig.6b. Testing was conducted to profile along two planes into the liner-rock system. One profile was along the springline and the other profile was near the crown as illustrated in Fig.6b. Testing in progress along an array near the crown is shown in Figure 6c.

The SASW testing program was designed to investigate the following: (1) thickness and quality of the concrete liner in the springline and crown areas, (2) thickness and quality of grout in the crown area, (3) identification of any voids in the crown area, and (4) the stiffness and variability of the rock behind the liner. (Grouting in the crown area was done after construction of the concrete liner.) The program successfully answered these questions. Due to space limitations, only results from one location along the springline are presented.

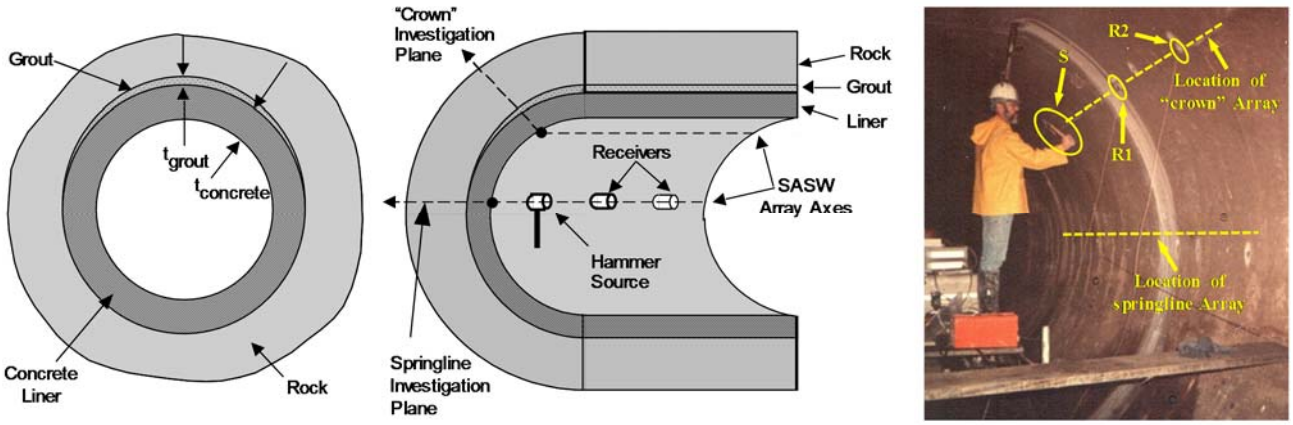

(a) Generalized tunnel cross-section showing concrete liner

(b) SASW testing arrangement and planes of investigation

(c) SASW testing : hammer source and accelerometer receivers

Fig. 6 – SASW testing performed inside a concrete-lined tunnel that was constructed in rock

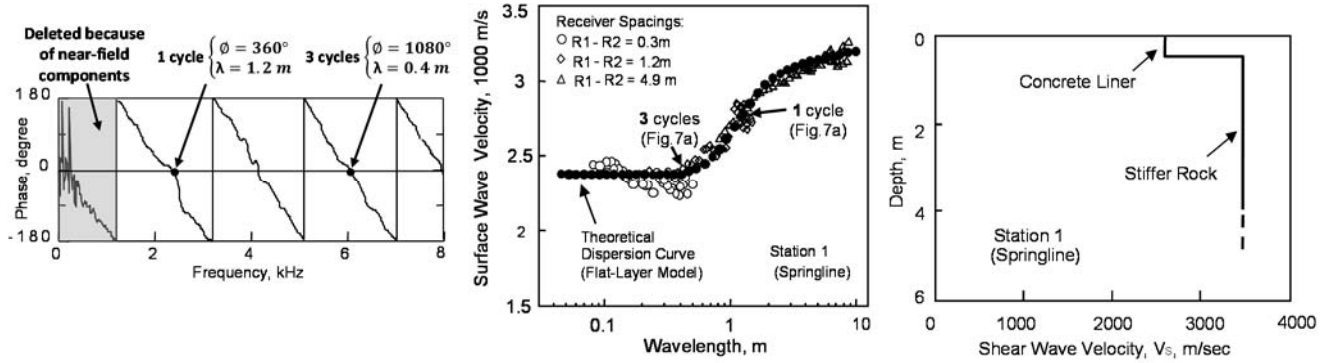

(a) Warpped-phase measurements; receiver-pair spacing = 1.2 m

(b) Forward modeling; field and theoretical dispersion curves

(c) V_S profile determined in concrete liner and rock

Fig. 7 – Examples of the wrapped-phase recorded in the field, composite field and theoretical dispersion curves, and resulting V_S profile in the concrete liner and host rock.

The wrapped phase determined with a pair of accelerometer receivers spaced 1.2 m apart are shown in Fig.7a. The results are excellent as shown by the continuous, "sawtooth" wrapped-phase relationship. The high wave velocities of both the concrete liner and surrounding host rock allowed a significant amount of high-frequency (f > 10 kHz) energy to be transmitted along the tunnel axis. As noted earlier, these results are viewed in the field during testing so that one can immediately judge how well the test is being conducted and determine if any adjustments to the testing procedure should be made.

The composite field dispersion curve at this location is shown in Fig.7b, with each portion of the curve identified according to receiver spacing. As seen in Fig 7b, only three receiver spacings were required to evaluate the liner and the rock immediately behind it. Wavelengths ranging from about 0.1 to 8 m were used. The fitting of the theoretical and field dispersion curves is also shown in Fig.7b. The resulting stiffness profile is presented in Fig.7c. The forward model used in these initial analyses was based on a flat, horizontally-layered model. (Subsequently, the analysis for a circular cavity with concentric layers was developed, and the theoretical dispersion curve is essentially the same as the curve shown.) The V_S profile in Fig.7c shows a high-quality concrete liner (V_S ~ 2500 m/s) that is about 30 cm thick. At this location, the liner is in direct contact with the rock (as was found at all test locations), and the rock is stiffer than the concrete at this location.

5. Example #3 – Stage Testing of a Test Fill to Predict the V_S Profile in a Deep Engineered Fill Before Construction

A test fill was constructed to estimate if a deep (28-m thick) engineered fill to be constructed with the same soil as the test fill would exhibit values of $V_S \geq 300$ m/s at a depth of about 12 m below the surface. The 12-m depth is the proposed depth of the bases of two nuclear islands in the deep engineered fill and one part of the seismic design of the nuclear power plants requires $V_S \geq 300$ m/s at this level. The test fill had plan dimensions of 6 by 18 m as shown in Fig.8a. A total of seven SASW arrays were tested at each of the four stages during construction of the test fill. The array centers are identified in Fig. 8a by letters A through G. The test fill was constructed with a silty sand using 23-cm loose lifts. Each lift was compacted to a density greater than 95% modified Proctor density. SASW testing at the four construction stages occurred when the test-fill thicknesses were nominally 1.5, 3, 4.5, and 6 m. SASW testing was performed using a bulldozer source and 4.5-Hz geophones. SASW testing in progress at Stage 2 (fill thickness about 3 m) is shown in Fig.8b.

The V_S profiles determined at Stage 2 and Stage 4 are presented in Figs.8c and 8d, respectively. All seven V_S profiles are shown in each figure along with some slightly deeper V_S measurements in the natural soil. (Note that a depth of 0 m in each figure represents the existing fill surface at that construction stage.) Clearly, all seven V_S profiles at each stage are nearly the same, with only small differences near (~ 1.5 m) the fill surface. A best-fit curve to the seven V_S profiles in each stage was added for comparison purposes. The four, best-fit V_S curves are presented in Fig. 8e. These four V_S profiles clearly illustrate how the small-strain stiffness of the silty sand in the

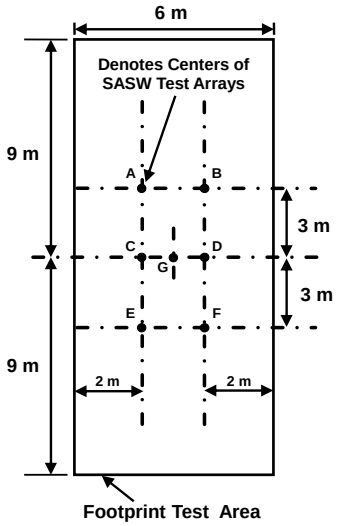

(a) Plan view of test fill with 7 SASW locations tested at each stage

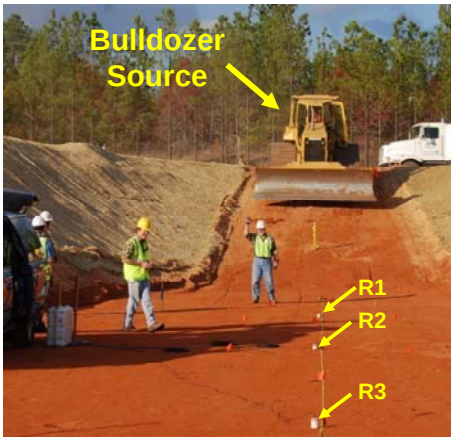

(b) SASW testing in progress at Stage 2; fill thickness ~ 3 m

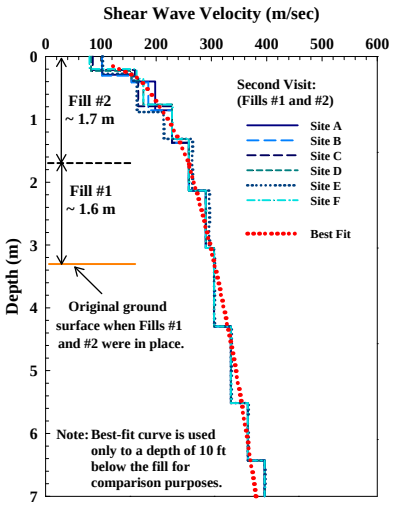

(c) Seven V_S profiles determined at Stage 2; fill thickness ~ 3 m

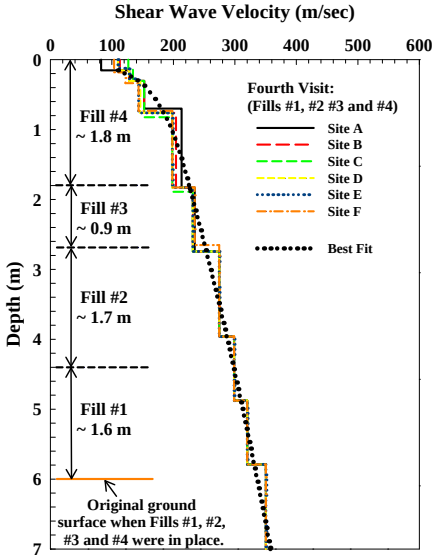

(d) Seven V_S profiles determined at Stage 4; fill thickness = 6 m

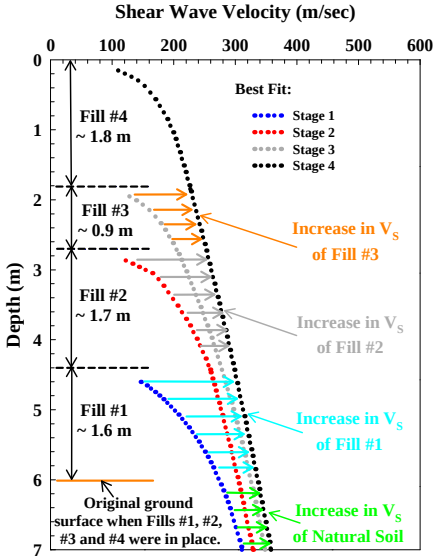

(e) Changes in best-ft V_S profiles from Stage 1 to Stage 4

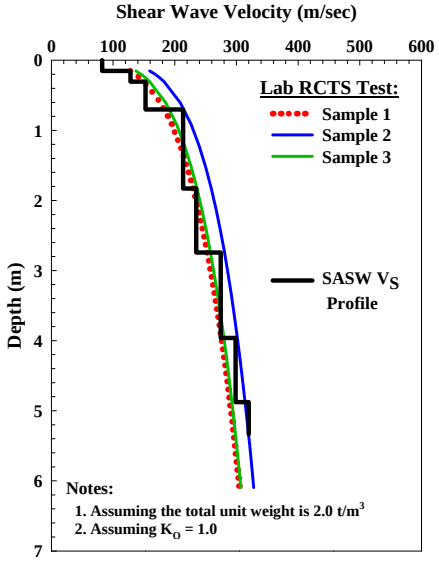

(f) Average V_S profile of test fill compared with laboratory V_S profiles from RC testing

Fig. 8 – SASW testing to determined V_S profiles in a test fill in stages during construction for use in predicting V_S values in a deep engineered fill before construction

test fill as well as the stiffness of the natural soil beneath the test fill increased as the test-fill thickness increased. Horizontal lines starting at initial best-fit curves of Stages 1, 2 and 3 and extending to the best-fit V_S profile for Stage 4 show how the stiffness of the soil in the lower stages increased with loading as the fill thickness increased.

An average V_S profile selected to represent the fill is presented in Fig.8f. This profile is also compared in Fig.8f with several V_S profiles determined by dynamic laboratory testing of fill specimens using the torsional resonant column (RC) method. The laboratory specimens were constructed with the same silty soil used in the test fill. The specimens were also constructed to the same density and water content as the fill. Three important points that are shown by the field and laboratory V_S profiles in Fig.8f are the following. First, extrapolation of the representative V_S profiles in the test fill demonstrates that V_S will be greater than 300 m/s at a depth of 12 m in the deep engineered fill. Second, the laboratory V_S profiles determined by torsional RC testing agree well with the

average V_S profile in the test. This close comparison was expected because both the test fill and laboratory soils represent the same soil that has been processed (compacted to the same density and water content) so that any depositional and aging effects have been removed. Third, close comparison between field and laboratory V_S measurements indicate that laboratory testing of other soils (for instance, a gravelly sand) could be used successfully to predict the stiffness of the fills constructed with different granular soils.

6. Example #4 – Deep V_S Profiling with Liqudator around Yucca Mountain, Nevada

About 35 years ago, Yucca Mountain, Nevada, was initially approved as the site for development of a geologic repository for high-level radioactive waste and spent nuclear fuel in the United States. The U.S. Department of Energy conducted studies to characterize the site and assess its future performance as a geologic repository. As part of these studies, a comprehensive program of deep seismic profiling was conducted around Yucca Mountain to evaluate the V_S structure of the repository block and adjacent areas where support facilities might be located. The resulting V_S data were used as input into the development of ground motions for the preclosure seismic design of the repository and for postclosure performance assessment. The SASW method was employed in the deep profiling which was defined as profiling to depths of 300 to 450 m.

Two key elements in successfully performing the deep V_S profiling at Yucca Mountain were the shear wave velocities of the rocks and the lowest frequencies generated by the active seismic source. Yucca Mountain consists of stacked layers of tuffs with V_S generally above 800 m/s at depths greater than 80 m. Therefore, profiling depths in these rocks will be more than twice the depths possible in moderately soft soils. The second key element is the low frequency range that can be generated by the active source. In this case, Liquidator (shown in Fig.3d) was an excellent source because frequencies as low as 1.0 Hz could be generated with this unique large vibroseis. Typically it was only possible to test one site per day due to the time required to deploy receivers over large distances (up to 1000 m) in rough terrain combined with the extended duration of the stepped-sine sweep (see Fig.3e) at low frequencies which require more than 45 minutes of constant shaking. Nevertheless, deep profiling was performed at a total of 17 sites.

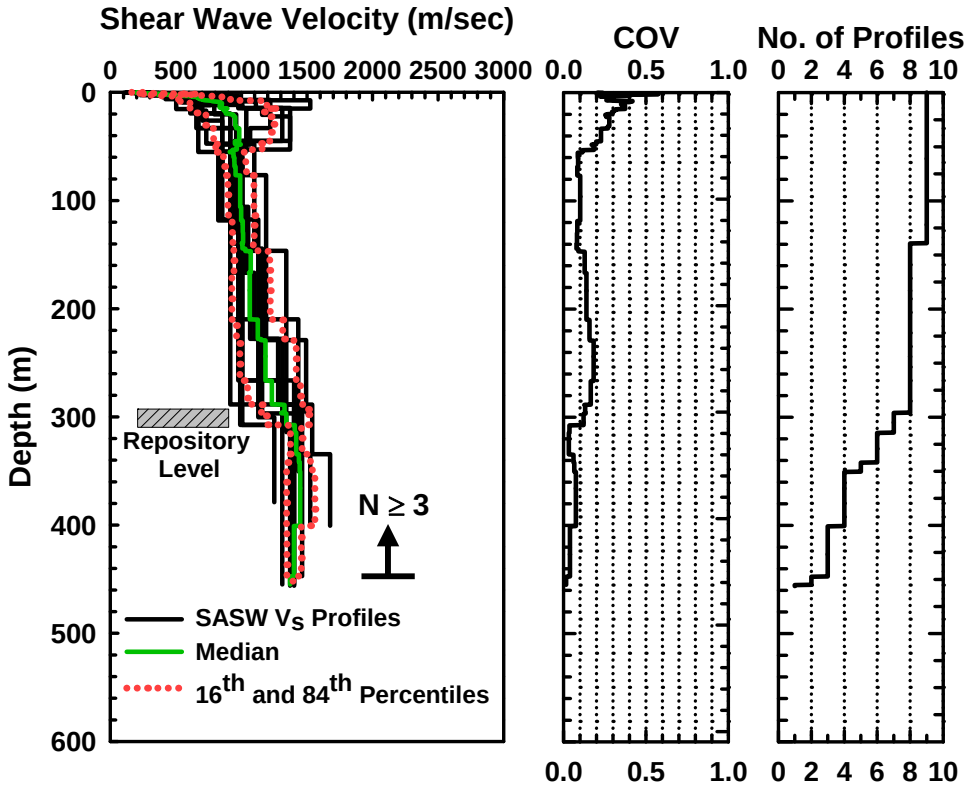

Fig. 9 – Statistical analysis of the 9 deep, V_S profiles in Group 1 at Yucca Mountain; small gradient in median V_S profile

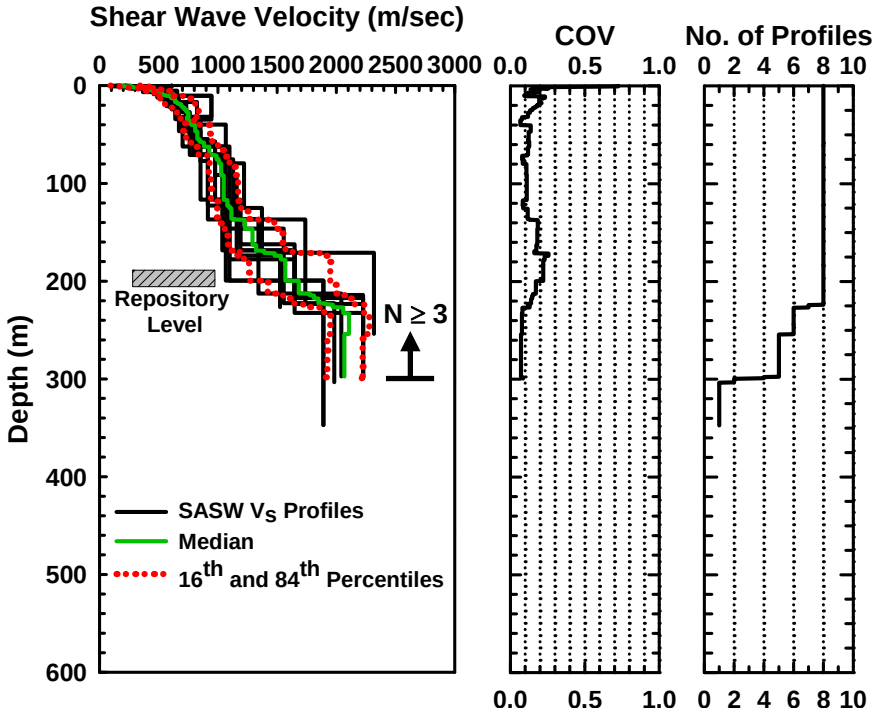

Fig. 10 – Statistical analysis of 8 deep, V_S profiles in Group 2 at Yucca Mountain; moderate gradient in median V_S profile and stiffer rock below 200 m

Once the V_S profiles of the 17 sites were determined, it became clear that the V_S profiles could be sub-divided into two groups The following statistical data were determined for each group: (1) median, 16th and 84th percentile profiles of V_S, (2) coefficient of variation (COV) which is equal to one standard deviation divided by the mean of the V_S profiles at each depth, and (3) the number of profiles (N) that were measured at each depth. The data sets for Groups 1 and 2 are presented in Figs.9 and 10, respectively. The first group, presented in Fig.9, has a smaller gradient in the median V_S profile and somewhat lower V_S values around the proposed repository level (depth about 300 m). The Group 2 profiles, presented in Fig.10, were located in a general area where the proposed repository level was shallower (about 200 m). The Group 2 V_S profiles exhibit a larger gradient and higher V_S values around the repository level compared to Group 1. It is also interesting to note that low COV values were evaluated over much of the profile for both groups, generally less than 0.13. The COV values increased to around 0.20 at depth in each group. The increased in COV values seem to be due more to the variations in the depth of the layer boundaries rather than variations in the velocities of adjacent layers.

7. Summary and Conclusions

The SASW seismic method is a nondestructive and noninvasive method of V_S profiling. The method is used in geotechnical, geophysical and seismological studies, particularly those involved in predicting the dynamic response of the built and natural environments during earthquake shaking. The basis for the method, field procedures and equipment, data analysis procedures and example V_S profiles are presented using four example projects. The projects range from shallow V_S profiling (depth < 5 m) of a concrete-lined tunnel for a forensic study to deep V_S profiling (depths from 300 to 450 m) of tuffs at Yucca Mountain, Nevada, for earthquake response studies. The four example projects demonstrate that the SASW seismic method is theoretically based, robust, and most helpful in terms of characterizing geotechnical and geological sites which also leads to generating a more comprehensive understanding of the material.

8 Acknowledgments

Any opinions, findings, and conclusions or recommendations expressed in this material are those of the authors and do not necessarily reflect the views of the Consortium of Organizations for Strong-Motion Observation

Systems (COSMOS) Facilitation Committee for the Development of the COSMOS International Guidelines for the Application of NonInvasive Geophysical Techniques to Characterize Seismic Site Conditions.

Numerous individuals and organizations have contributed to this work over the past several decades. Just to name some of the individuals, they include: Marwan Aouad, James Bay, Brady Cox, Cecil Hoffpauir, Min Jae Jung, Asli Kurtulus, Alan Lancaster, Michael Lewis, Yin-Cheng Lin, Farn-Yuh Menq, Soheil Nazarian, Glenn Rix, Julia Roberts, Jose Roesset, Brent Rosenblad, Michael Schuhen, Jeff Smith, Andrew Valentine, Ivan Wong, and Jiabei Yuan. Thanks goes to these individuals and multiple organizations.

9 Copyrights

10 References

[1] Nazarian S, and Stokoe KH, (1984): In situ shear wave velocities from spectral analysis of surface waves. 8th *World Conference on Earthquake Engineering*, (3), 31-38, Prentice-Hall, San Francisco, CA.

[2] Stokoe KH, and Nazarian S (1985): Use of Rayleigh waves in liquefaction Studies, in, R.D. Woods, ed., "Measurement and use of shear wave velocity for evaluating dynamic soil properties." ASCE, New York.

[3] Richart FE, Woods RD, and Hall JR (1970): Vibrations of Soils and Foundations. Prentice Hall, Englewood Cliffs, 414, New Jersey.

[4] Kausel E, and Roesset JM (1981): Stiffness matrices for layered soils. *Bulletin of the Seismological Society of America*, **71**, 1743-1761.

[5] Stokoe KH, Wright SG, Bay JA, and Roesset JM (1994): Characterization of geotechnical sites by SASW method. *ISSMFE Technical Committee 10 for XIII ICSMFE*, Geophysical Characteristics of Sites, A.A. Balkema, Rotterdam & Brookfield, Netherlands, 785-816.

[6] Joh SH (1996): Advances in the data interpretation technique for Spectral-Analysis-of-Surface-Waves (SASW) measurements. Ph.D. Dissertation, The University of Texas at Austin, 240.

[7] DiGiulio G, Savvaidis A, Ohrnberger M, Wathelet M, Cornou C, Knapmeyer-Endrun B, Renalier F, Theodoulidis N, and Bard PY (2012): Exploring the model space and ranking a best class of models in surface-wave dispersion inversion: Application at European strong-motion sites. Geophysics, **77**, 147–166.

[8] Cox BR, and Teague D (2016): Layering ratios: A systematic approach to the inversion of surface wave data in the absence of A-priori information. Geophysical Journal International, 207, 422–438.

[9] Lin LY, Stokoe KH, Rosenblad B, (2008): Variability in V_S profiles and consistency between seismic profiling methods: A case study in imperial Valley, California. *3rd International Conference on Site Characterization (ISC-3)*, Taipei.

[10] Foinquinos MR (1991): Analytical study of inversion for the spectral analysis of surface waves method. Master's Thesis, The University of Texas at Austin, 119.

[11] Roesset JM, Chang DW, and Stokoe KH (1991): Comparison of 2D and 3D models for analysis of surface wave tests. *5th International Conference on Soil Dynamics and Earthquake Engineering*, 111-126.

[12] Lin YC, Joh SH and Stokoe KH (2014): Analyst J: Analysis of the UTexas 1 surface wave dataset using the SASW methodology. ASCE, Geo-Congress, Atlanta, Georgia.